Spectrum of Engineering Sciences
ISSN (e) 3007-3138 (p) 3007-312X Volume 3, Issue 4, 2025

IMPACT ON COMPUTATIONAL DIESEL SPRAY MODELS BY EVAPORATING AND NON-EVAPORATING CONDITIONS

Aftab Ahmed Soomro[*1], Asmatullah[2], Safiullah[3], Basit Ahmad[4], Muhammad Nouman[5]

[*1, 2]*Department of Mechanical Engineering Technology, Benazir Bhutto Shaheed University of Technology and Skill Development, Khairpur Mirs, Sindh, Pakistan*
[3]*UCI Combustion Laboratory, University of California, Irvine, CA, USA*
[4]*Department of Electrical Engineering, NFC Institute of Engineering and Technology Multan, Pakistan.*
[5]*Department of Electrical Engineering, Bahauddin Zakariya University Multan, Pakistan*

[*1]aftabsoomro@bbsutsd.edu.pk , [2]asmatmemon@bbsutsd.edu.pk , [3]safiull@uci.edu, [4]basitahmad3884@gmail.com, [5]engineer.muhammad.nouman@gmail.com

DOI: https://doi.org/10.5281/zenodo.15194820

Keywords
Evaporating, Non-evaporating Models, Spray, CFD, simulation, Diesel Engine.

Article History
Received on 03 March 2025
Accepted on 03 April 2025
Published on 11 April 2025

Corresponding Author: *
Aftab Ahmed Soomro

Abstract

This study explores the impact of diesel spray computation models and their constants by varying the parameters. Various enabled and disabled evaporating models based on changing the parameters i.e tip penetration, angle of inclination, evaporation ratios and spray shapes are compared with the experimental data to get their results. A viable automotive diesel injector was used in the experiments having nozzle diameter of 0.122mm. Sprays were injected with a pressure of 140 MPa. The measurements are taken of evaporating and non-evaporating spray in a high-pressure high-temperature constant volume vessel by adjusting ambient conditions. Simulation were taken of computational sprays using an Eulerian-Lagrangian two-phase fluid framework in a hexahedron cylindrical mesh box. The inputs including initial spray, rate of injection and angle of inclination were measured for the Computational Fluid Dynamics (CFD) simulation including with experimental methods. A systematic approach was used by enabling and disabling the various breakup models including primary, secondary and evaporation models for evaluation purpose. The results were demonstrated for secondary breakup models and their constants significantly influence the accuracy of spray predictions at non-evaporating conditions. While upon evaporation model the evaporating spray of droplet plays a crucial role in shaping the liquid penetration and evaporation ratios. This study provides intuitions into the importance of tuning model constants to achieve promising approach with experimental data, offering guidelines for improving diesel spray modeling in computational fluid dynamics (CFD) simulations.

INTRODUCTION

The energy efficiency is the crucial global demand as well as to control its impact on the environmental health. In this regard the research approach follows the strict emission regulations by optimizing the fuel spray characteristics in diesel engines. Diesel combustion is extremely dependent on fuel atomization, disintegration of droplets, and vaporization, which effects the ignition delay, combustion efficiency, and pollutant formation [1-2]. The spray dynamics can improve fuel-air mixing ratio,

leading to improve combustion efficiency and reduce emissions like carbon monoxide (CO), nitrogen oxides (NOx), and particulate matter [3-5].

Computational Fluid Dynamics (CFD) is a powerful tool that can be used in spray modeling and simulating, providing the behavior of fuel atomization and vaporization. The accuracy of CFD predictions depends upon the selection and tuning of numerical models. It governs the primary and secondary fuel disintegration, evaporation, and turbulence. The primary breakup model make initial disintegration of the liquid jet, while the secondary breakup model governs additional fragmentation of droplets into smaller sizes, affecting spray penetration and angle of inclination [6-8]. Similarly, evaporation models control the rate of liquid fuel transitions to the vapor phase, prompting the mixture formation and combustion efficiency [9-10].

The aim of this study is to evaluate the effects of unlike breakup model and evaporation models on diesel spray behavior systematically. The research focuses on two key conditions: evaporating and non-evaporating sprays. Experimental data acquired using a high-pressure, high-temperature constant volume chamber serve as a benchmark for confirming CFD simulations. A commercial diesel injector is used in the experiments having nozzle diameter of 0.122 mm and an injection pressure of 140 MPa. The computational setup employs two-phase approach of an Eulerian-Lagrangian with spray parameters comprising rate of injection and initial spray angle derived from experimental measurements.

The study investigates the influence of primary Injection and secondary breakup models, including the Kelvin-Helmholtz Rayleigh-Taylor (KHRT) [11], Wave [12], and Taylor Analogy Breakup (TAB) [13] models, along with different evaporation models such as Dukowicz (Dukow.) [14] and Frolov[15]. The objectives of study is to determine the optimal combination of numerical methods for accurate spray prediction by enabling and disabling these models and adjusting key constants of model.

Findings from this study emphasized the crucial need for selecting proper breakup and evaporation models tailored to specific spray conditions, varying the results depends on differing spay characteristics. For non-evaporating sprays, the predicting of spray penetration and angle depends on secondary breakup models and their constants. While in evaporating conditions, the selection of evaporation model affects liquid penetration and evaporation ratios. The results provide valuable guidelines for improving diesel spray modeling in CFD simulations, contributing to the development of more efficient and cleaner combustion systems.

2. Methodology

CFD simulation computational methods are explained in this section. The experimental data of evaporating and non-evaporating diesel sprays are taken from previous publication [16].

2.1 Experimental Conditions:

Experimental conditions are shown in Table 1. A profitable automotive diesel injector was used having a nozzle diameter of 0.122mm. The sprays were measured at 140 MPa. That was the maximum injection pressure by which the laser absorption and scattering (LAS) tracer fuel injected. While the pressure slightly increased resulted in the solidification of fuel. The injection quantity was maintained at 5mm^3. Sprays are compared based on evaporating and non-evaporating conditions. The evaporating condition is simulated at the room temperature while the non-evaporating condition is experimented at 770^{o}C. The selection of such temperatures was to maintain the nitrogen density i.e. 16kg/m^3 mimicking the real-time diesel engine condition.

Table 1 Experimental Conditions

Injection Conditions		
Injector Type	Mini Sac Piezo	
Number of Nozzle Holes	1	
Umbrella Angle (deg)	0	
Nozzle Hole Diameter (mm)	0.122	
Injection Pressure (MPa)	140	
Injection Quantity/1hole [mm^3]	5	
Ambient Condition	Non-Evaporating	Evaporating
Gas	Nitrogen (N_2)	
Pressure [MPa]	1.4	3.6
Temperature [K]	Room	770
Fuel	Diesel	Tracer Fuel (97.5% n-tridecane, 2.5% -MN)
Density [kg/m^3]	16	

2.2 Computational mesh

Diesel spray experimental results were validated with the computational simulation using AVL FIRE commercial CFD software. The simulation was carried out in a simple hexahedron cylindrical mesh box with the mesh size of 475,200 cells. The length and the radius (L +B) of the spray box were set to 0.1 m and 0.02 m, respectively. Three boundary conditions were set using selections option. The sides and the top of the spray box were declared as wall, whereas the bottom was declared as a non-reflecting outlet. The spray box mesh is shown in Figure 1.

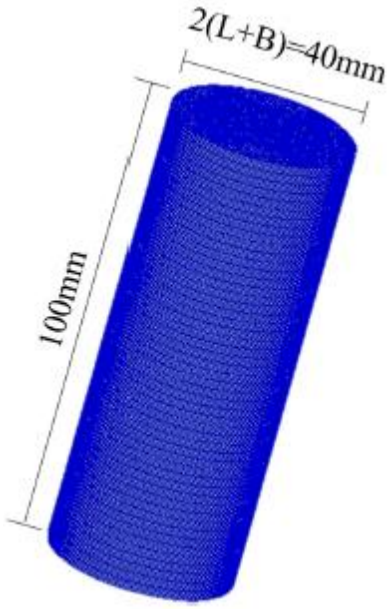

Figure 1: Spray Box Mesh

2.3 Cases Studies and Model Constants

In this section, computational conditions based on the cases studied are explained. As mentioned previously, this work performs a parametric study on primary breakup model (P.M), secondary breakup model (S.M) and evaporation model (E.M), hence Table 2 and Table 3 are depicting all cases and models. Case 1 is used as a baseline condition which will be used to compare with other cases. All model constants are shown in Appendix.

Table 2 Models and Cases Studied

	Case 1	Case 2	Case 3	Case 4	Case 5
P.M	Deact.	Core Inj.	Core Inj.	Deact.	Deact.
S.M	KHRT	KHRT	Deact.	Wave	TAB
E.M	MultiC	MultiC	MultiC	MultiC	MultiC

Table 3 Breakup Length Constant (C2)

	Case1	Case1a	Case1b	Case1c	Case1d	Case1e	Case4a
C2-KHRT	12	20	30	40	50	60	12
C2-Wave	-	-	-	-	-	-	12

2.4 Inputs for CFD Simulation

Based on previous research, it was found that the Injection Rate (IR) and initial spray angle are fundamental in predicting the spray tip penetration and spray angle. Therefore, the selection and measurement of these quantities are always critical. In this work, a raw IR transient profile was measured with Zeuch method and was processed with a 5 kHz Butterworth low pass filter. On the contrary, the initial spray angles are extracted from highly magnified spray images near the nozzle hole. The angles were measured at 1mm downstream distance. Figure 2 shows IR and initial spray angle profiles.

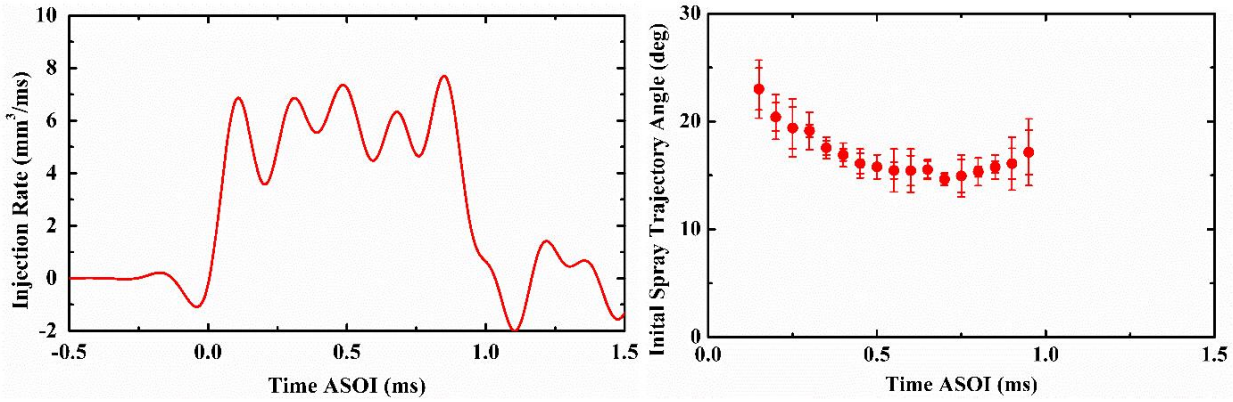

Injection Rate Initial Spray Angle

Figure 2: Injection Rate and Initial Spray Trajectory Angle Profiles

3. Results and Discussion

3.1. Activating Primary Breakup Model

In spray morphology, the first phase of atomization is termed as primary breakup where fuel droplets start to break. Here, the Core Injection Primary breakup model with default model constants set by AVL FIRE is chosen. The primary breakup model with the same models to Case1 is activated in Case2, while in Case 3, the primary breakup model is activated, and the secondary breakup model was disabled.

Spray Shapes at 0.6ms After Start of Injection (ASOI), Spray tip penetration and spray angle under non-evaporating condition of Case1, Case2 and Case3 are compared with experiment in Figure 3. In this study, experimental spray shapes are shown after subtracting background; whereas simulation spray structures are illustrated based on the droplet diameter. In each image of spray structure is shown the droplet size and color contour. Moreover, the graphical representation of experimental results "exp" is shown with symbols, while the numerical results "sim" are indicated with solid lines. From Figure 3, Case1 shows larger droplet size near nozzle field due to deactivation of primary breakup model. However, when the primary breakup model is activated i.e. in Case2 and Case3, the droplet size is significantly reduced especially near nozzle hole. The deactivation of primary breakup model forces computational approach to assume the initial droplet size equal to its nozzle diameter. Practically, the initial droplet may not be as large as nozzle diameter, yet its size is larger compared to droplet size in the

secondary breakup region. Thus, a reasonable assumption is taken in Case 1. In Case3, the secondary breakup model is turned off; therefore, the same droplet size from the nozzle tip region to the spray tip is witnessed; hence, the importance of secondary breakup modeling could be understood. When talking about the spray tip penetration, Case2 and Case3 comply perfectly with the experiments, however, due to their narrow sprays, the spray angle comparison is quite poor.

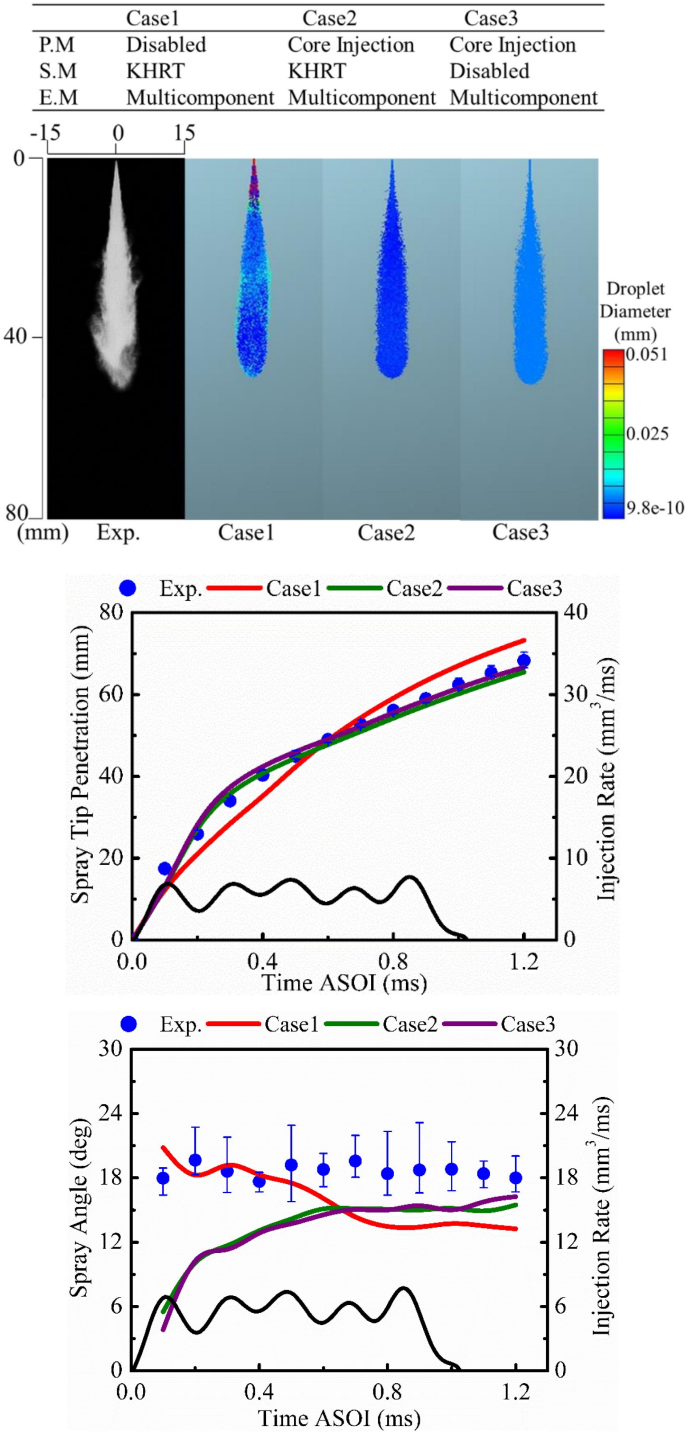

Figure 3: Sprays Characteristics Comparison under Non-Evaporating conditions

Evaporating results including spray tip penetration (liquid + vapor) and evaporation ratios are compared in Figure 4. Understanding that the evaporating spray experiment and CCD camera image capturing combination requires an ample time between two injection events; thus, three timings (i.e. 50% ASOI, 0.1ms after End of Injection (EOI) and 0.2ms after EOI) per injector were chosen. Moreover, to eliminate the measurement error, the spray experiment per single injection timing was repeated three times and results shown are arithmetic mean of those three trials. In experiments the liquid penetration is observed during the injection period only; and it disappears soon after the end of injection, within short interval time of 0.1ms. It indicates that the liquid fuel evaporates completely when injection period is finished and is ready for combustion. In simulation comparison, the liquid penetration of Case1 and Case2 are almost identical because of their smallest mean droplet size. However, at 0.1ms AEOI, the liquid penetration could be still witnessed; thus, an overestimation of numerical work is assumed. While, the vapor penetration, like spray tip penetration in non-evaporating condition, is predicted correctly by Case2 and Case3 after End of Injection (EOI) period. On the contrary, evaporation ratio, in this study, is defined as the ratio of evaporated fuel mass to the injected fuel mass. Experimental data shows 100% evaporation ratio after the injection period; which supports the claim that the liquid fuel evaporated after EOI period. Case1 shows a qualitative and quantitative agreement with experiments; however, the overestimation of Case2 is obvious because of its smallest droplet size in non-evaporating condition. Case2 is recommended when the spray simulation is assisted by the injector's internal flow simulation. Because, the primary breakup region is always influenced by the injector's internal flow including cavitation. The spray simulation, however, doesn't consider effects of the cavitation.

	Case1	Case2	Case3
P.M	Disabled	Core Injection	Core Injection
S.M	KHRT	KHRT	Disabled
E.M	Multicomponent	Multicomponent	Multicomponent

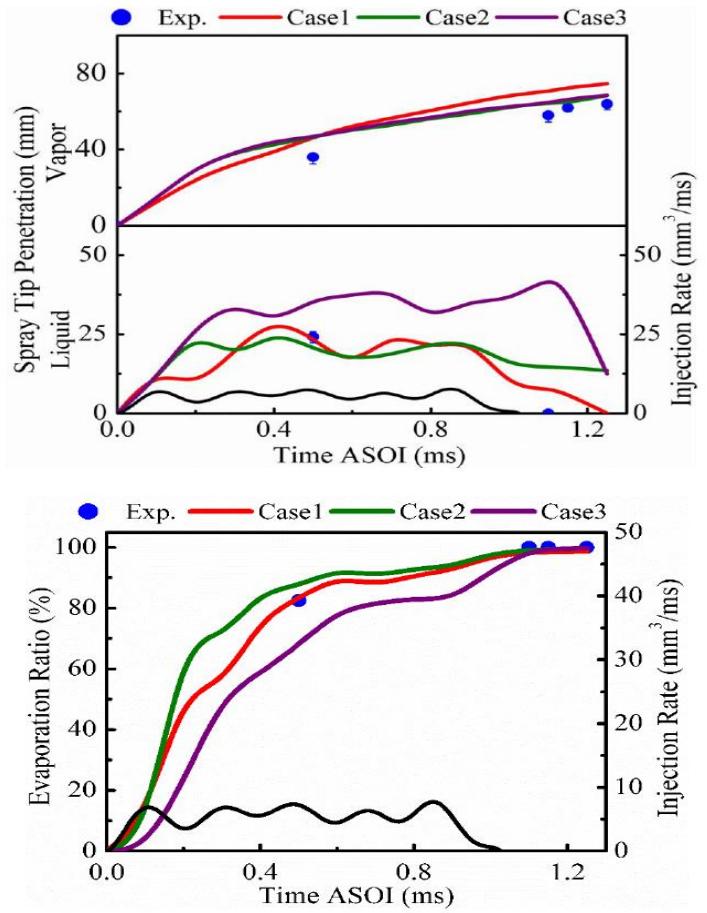

Figure 4: Evaporating Spray Tip Penetration and Evaporation Ratios

3.2 Activating Different Secondary Breakup Models

The importance of secondary breakup model could be seen from above results, i.e. Case3 when the secondary breakup model was deactivated, the breakage of large droplets into smaller ones could not be witnessed; thus, an illogical and impractical behavior of sprays was observed. In this section, different secondary breakup models with default constant set by AVL FIRE are activated. Apart from KHRT breakup model in Case1, WAVE and TAB breakup models are activated in Case4 and Case5, respectively.

Figure 5 shows experimental spray shapes at 0.6ms ASOI, spray tip penetration and spray angle comparison with simulation Case1, Case4 and Case5. The droplet size in Case4 at primary and secondary droplet breakup is significantly larger than Case1 and Case5. When talking about the comparison with Case1 and understanding that the KHRT model combines WAVE and RT models, the higher value of WAVE C2 is one of the primary reasons of larger droplet size, because it influences the wave growth rate, leading to less breakup and larger droplets. Since C2 corresponds to the droplet breakup time, $\tau_b = \frac{3.6C2R_d}{\Omega_{KH}\Lambda_{KH}}$, if this value is larger, the droplet breakup time would increase; thus, the droplet size would be large too. On the other hand, larger droplets are seen in the spray tip region of Case5; however, there's no any evidence of gradually decrement of droplet size, as seen in Case1 and Case4. It is due to the fact that, TAB model is based on the single droplet breakup phenomenon. The

spray tip penetration of Case5 is in good coordination with experimental results, whereas the deviation in Case1 and Case4 is clear. Moreover, a poor prediction of spray angle is witnessed for Case4 and Case5.

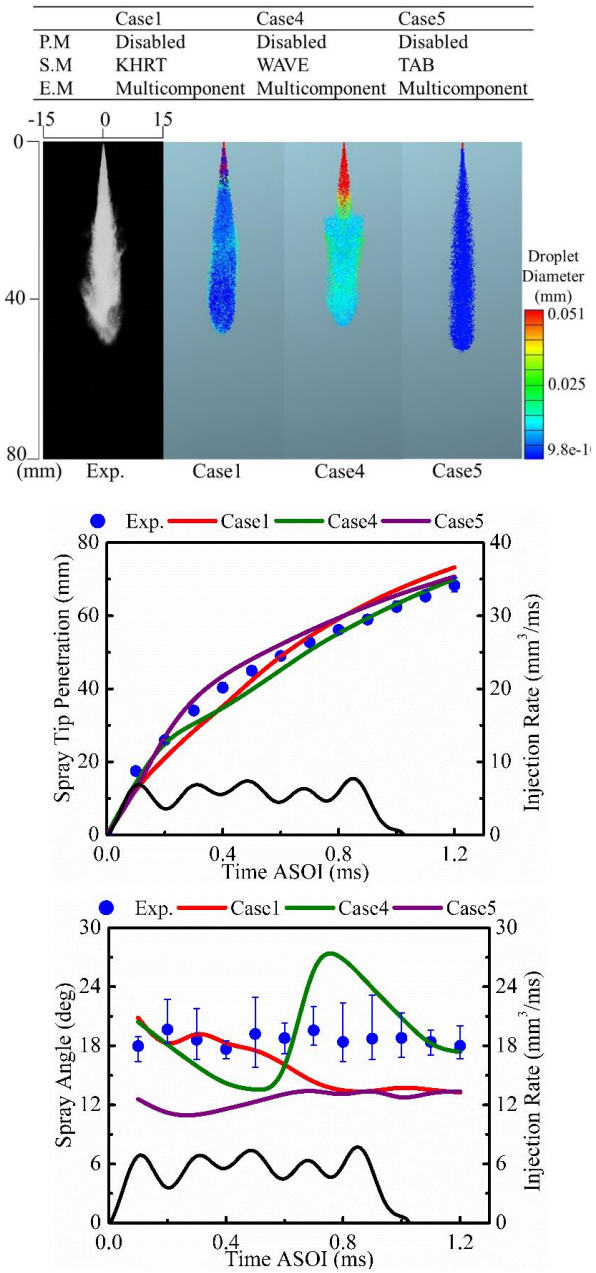

Figure 5: Sprays Characteristics Comparison under Non-Evaporating conditions

Evaporating results including liquid and vapor tip penetration and evaporation ratios are presented in Figure 6. The liquid penetration, using WAVE breakup model in Case4, shows an overestimation to the experimental results before and after the end of injection period probably due to the mean larger droplet size in the spray cloud. Also, the equilibrium state between spray propagation and droplet evaporation couldn't be achieved throughout the injection period, like seen for Case1 and Case5. Similarly, the vapor penetration results of Case4 resemble with experiments till the midstream of the injection duration; however an overestimation is

seen after EOI period similar to Case1 and Case5. Coming to the evaporation ratio comparison, the simulation results of Case1 and Case5 are identical and show good agreement with experiments, although the evaporation ratio is not 100% at after EOI in both these scenarios. Case4 shows a poor disagreement with experiments results due to its longer breakup time. The evaporation of droplet, when its size is larger, takes a longer time than one whose size is smaller i.e. Case1 and Case5. Interestingly, the spray behavior using TAB model in Case5 seems quite similar to Case2, when Core Injection primary breakup and KHRT secondary breakup models were turned on. Thus, if the spray angle is not a matter of concern, either Case2 or Case5 should be used.

	Case1	Case4	Case5
P.M	Disabled	Disabled	Disabled
S.M	KHRT	WAVE	TAB
E.M	Multicomponent	Multicomponent	Multicomponent

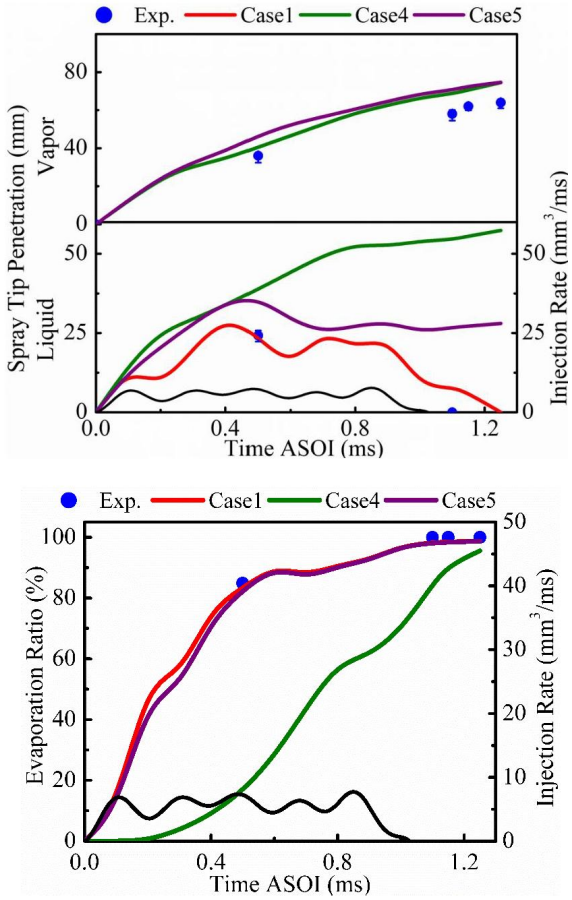

Figure 6: Evaporating Spray Tip Penetration and Evaporation Ratios

3.3 Altering Model Constants of KHRT Breakup Model

As seen earlier, when WAVE breakup model Case4 used larger C2 value the, spray results including spray tip penetration, spray angle, liquid and vapor penetration and evaporation ratio disagreed with experiments. Thus, this section shows the detailed view of C2 effect on the spray results when it is altered for KHRT breakup model. Shown in Appendix, the recommended value of C2 is from 5-60, thus, it is varied from 12 (Case1) to 60 (Case1e). All other models are similar to Case1, only the C2 value is altered.

Experimental spray shapes at 0.6ms ASOI, spray tip penetration and spray angle are compared with simulation Case1, Case1a, Case1b, Case1c, Case1d and Case1e, under non-evaporation condition, in Figure 5. With increasing the C2 value, larger droplets are seen in the spray cloud which

corresponds to the longer breakup time. Larger droplets cause longer spray penetration initially due to higher inertia forces of the larger droplets. However, when the spray momentum reduces in the quasi-steady state, the larger droplet tends to move in radial direction rather than the axial direction. The evidence of longer penetration at the initial stage of injection could be seen in the spray tip penetration graph of Figure 6. Whereas, the radial dispersion of spray in the radial direction could be understood from the spray angle comparison.

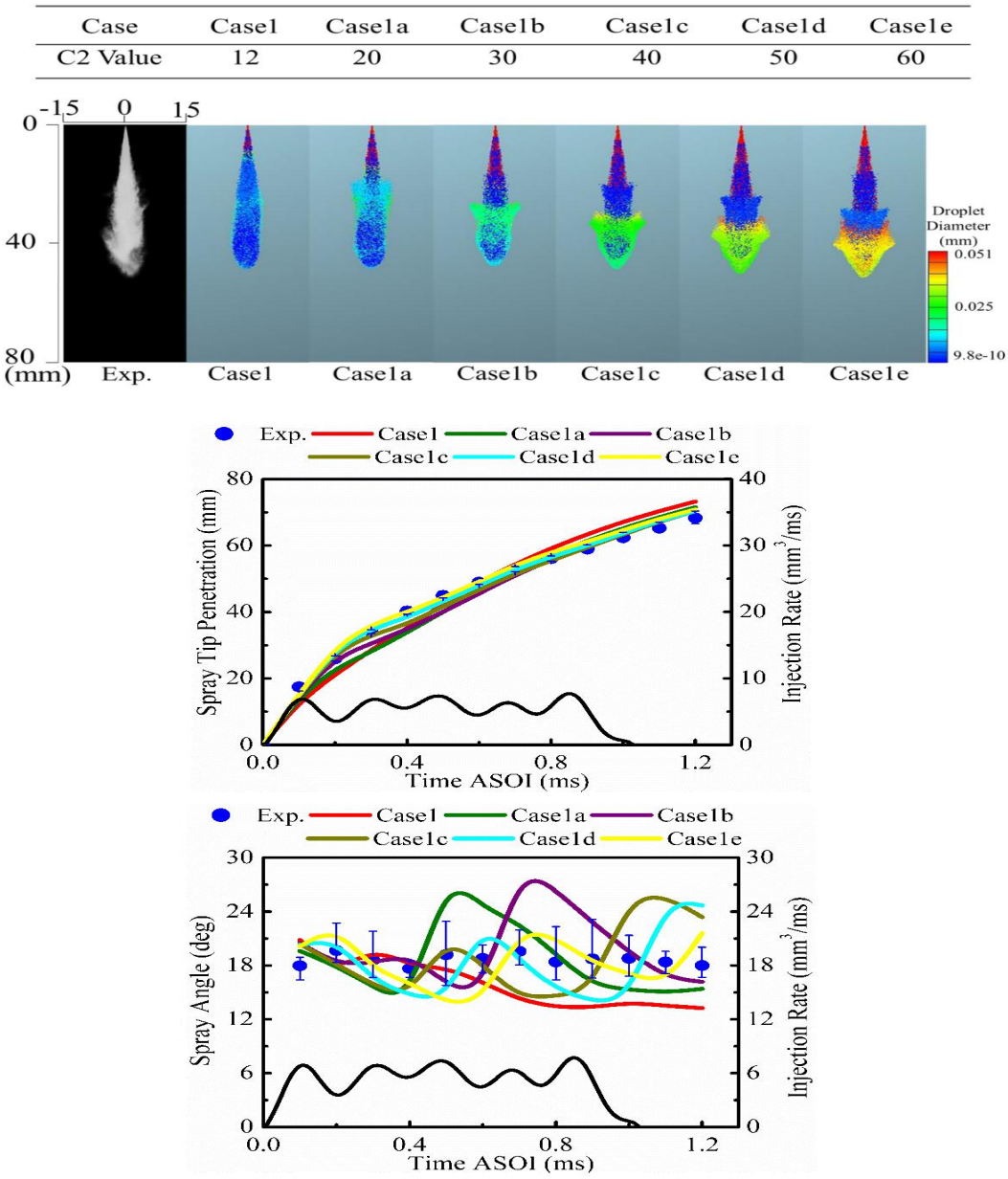

Figure 6: Sprays Characteristics Comparison under Non-Evaporating conditions

Evaporating liquid and vapor penetration and evaporation ratio of Case1, Case1a, Case1b, Case1c, Case1d and Case1e are compared with experimental results in Figure 7. The longer liquid penetration of all cases with larger C2 value was expected since the evaporation of larger droplets take certain time. The equilibrium state between spray propagation and droplet evaporation is only seen when C2 value is 20 or below it, i.e. Case1 and Case1a. Apart from them, all other cases show a very poor display of comparison. Vapor penetration results of simulation illustrate almost identical comparison in all cases.

Due to larger droplets, the evaporation becomes week; thus, when C2 value is larger, for example 60 in Case1e, only liquid penetration with only a few vapor around the spray periphery is considered. On the other side, in the evaporation ratio comparison, lowest C2 value (Case1) shows largest evaporation ratios while the larger C2 value shows a poor evaporation. As discussed earlier, larger droplets size accompanied with longer breakup time reduces droplet evaporation; in this case, an underestimation of Case1a to Case1e evaporation ratios was expected, The larger C2 value is suggested when the spray tip penetration is desirable; however, for diesel engines where droplet evaporation is key, smaller C2 value must be used for the engine combustion simulation.

Case	Case1	Case1a	Case1b	Case1c	Case1d	Case1e
C2 Value	12	20	30	40	50	60

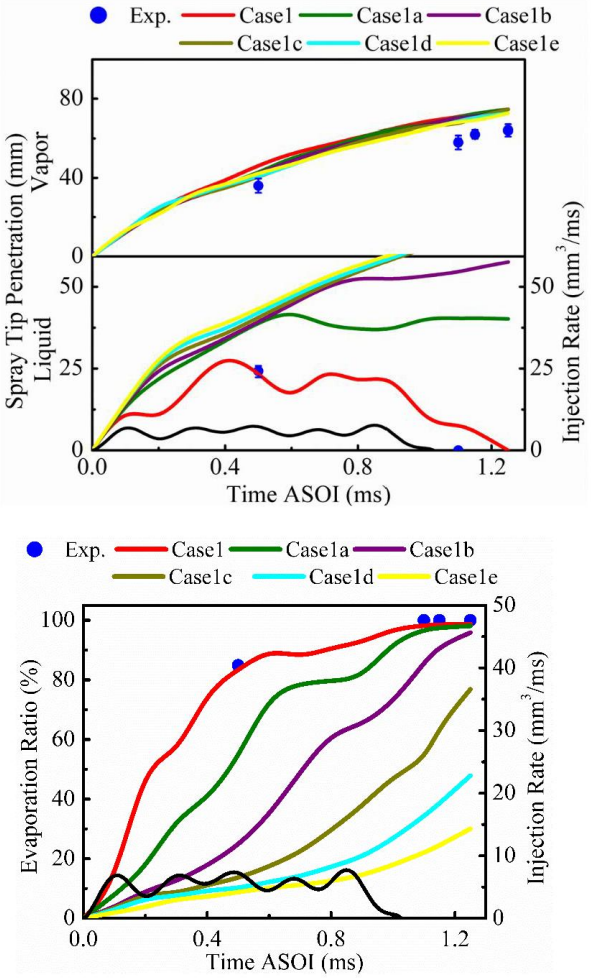

Figure 7: Evaporating Spray Tip Penetration and Evaporation Ratios

3.4 Altering Model Constant of WAVE Breakup Model

In this section, the C2 value of WAVE breakup model is altered to 12, same with Case1, and non-evaporating and evaporating results are compared with experiments and Case1.

Experimental spray shapes at 0.6ms ASOI, spray tip penetration and spray angle comparison with simulation Case1 and Case4a, under non-evaporating condition, is illustrated in Figure 8. Case4a shows larger droplets in the spray cloud even though the same value of C2 is used with Case1. The WAVE model is suitable for low to middle injection pressures; thus, the instability in droplet breakage is quite obvious at high injection pressures. Spray tip penetration comparison of Case1 and

Case4a is nearly identical, because the distance the spray reaches is similar for both cases. However, in the spray angle, Case4a exhibits relatively good quantitative agreement with experiments. As seen in the spray structure images that the larger droplets in Case4a disperse in the radial direction at the distance of around half of the penetration length. Near the nozzle field region, the spray momentum is larger; this momentum reduces far field when the spray propagates. Droplets with larger diameter, with lower axial injection momentum, disperse in the radial direction due to higher inertia mass. Thus, the Case4a shows greater spray angle.

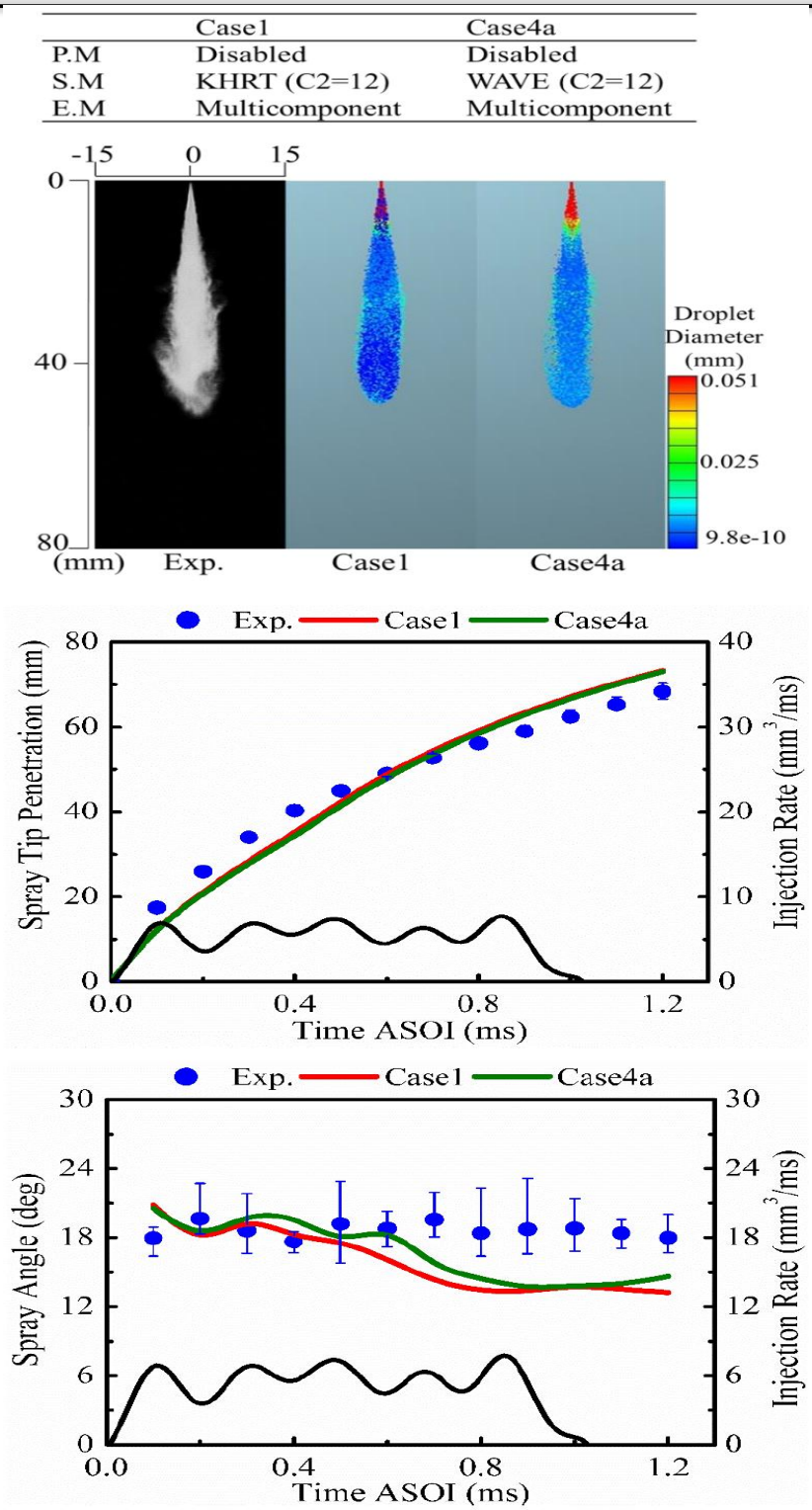

Figure 8: Sprays Characteristics Comparison under Non-Evaporating conditions

Evaporating liquid and vapor penetration and evaporation ratio of Case1 and Case4a are compared with experimental results in Figure 9. A longer liquid penetration of Case4a is seen, as expected, due to larger droplet size, although an equilibrium state is achieved at the same time to Case1. The vapor

penetration, unsurprisingly, is same for both cases since the spray tip penetration was similar under non-evaporating condition. On the contrary, the evaporation ratio is lower for Case4a due to larger droplet size. Thus, KHRT breakup model is highly recommended when fuel is injected with higher injection pressure.

	Case1	Case4a
P.M	Disabled	Disabled
S.M	KHRT (C2=12)	WAVE (C2=12)
E.M	Multicomponent	Multicomponent

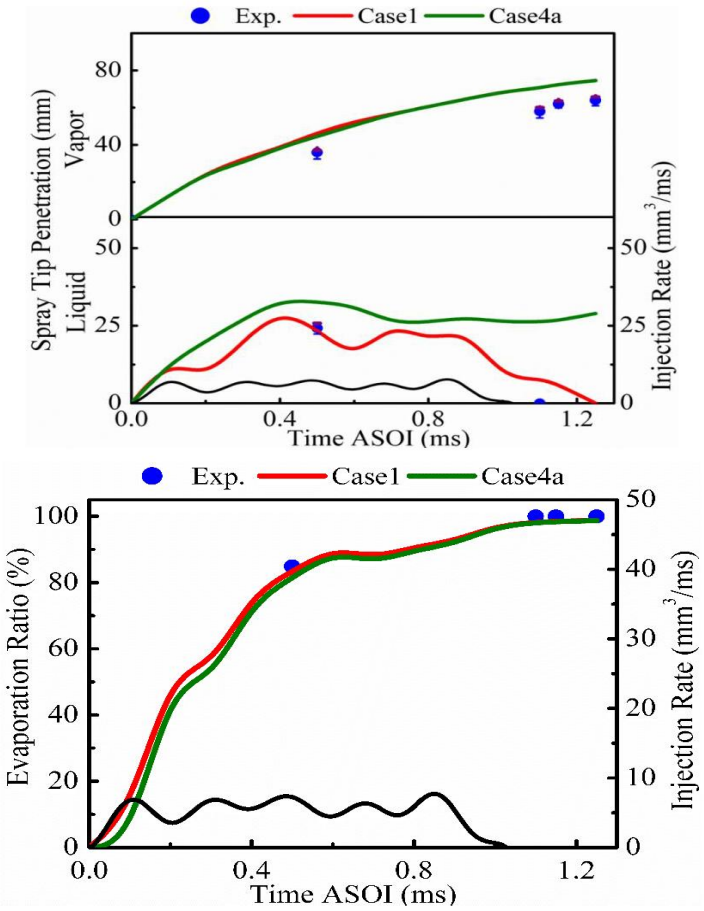

Figure 9: Evaporating Spray Tip Penetration and Evaporation Ratios

4. Conclusion and Recommendations

The effects of different models and model constants investigated and results were obtained under non-evaporating condition including spray shapes, spray tip penetration and spray angle. While under evaporating condition spray tip penetration (liquid+vapor) and evaporation ratio were compared with experimental data with predefined baseline condition. These models were activated and deactivated based on the baseline condition, which serves as a reference point for measuring changes and summarizing the following results, allowing for comparison and tracking of progress or deviations:

1. Activation of primary breakup model in combination with the secondary breakup model shortens droplet breakup time, leading to smaller droplets are found into the spray cloud, because initial breakup creates larger droplets than further broken down into the secondary smaller droplets as shown in Figure 10. This combination predicts spray tip penetration perfectly; however, it underpredicts spray angle and over predicts evaporation ratio.

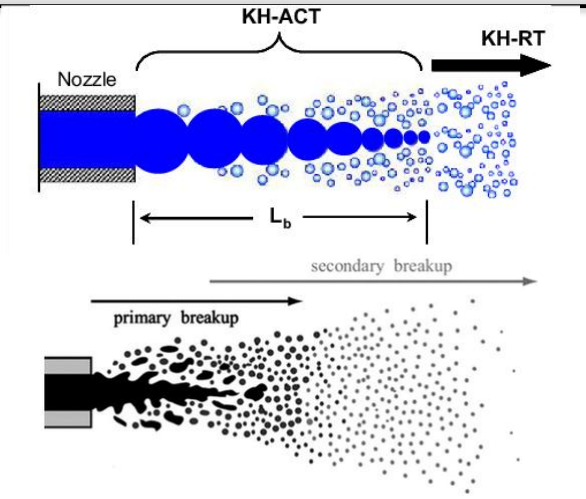

Figure 10: Primary and secondary breakup models [17]

2. TAB breakup model shows mimics the primary+secondary breakup model combo since the TAB model is developed on the single droplet dynamics phenomenon. Conversely, the WAVE model shows poor agreement with experimental observations in terms of spray angle, liquid penetration and evaporation ratio.
3. Changing the evaporation model doesn't show any clear effect on the non-evaporating spray as the droplet evaporation is very slow, because evaporation itself is not a primary factor. However, under evaporating condition, Dukowicz model accurately predicts experimental results but this model is only valid for single component fuels.
4. Increasing C2 model constant of KHRT can improve spray tip penetration results; however, the other properties such as spray angle, liquid penetration and evaporation ratio leading to disagreement in predictions.
5. Even though the C2 constant of WAVE breakup model is tuned based on the KHRT model, WAVE model shows larger droplet size, longer liquid penetration and lower evaporation ratios than that of the KHRT breakup model and experiments. This confirms that the WAVE breakup model is not suited for higher injection pressures.

Based on above search results, the baseline condition exhibits practical behavior of fuel spray is in good agreement with experimental results qualitatively. Therefore, it is recommended that, the chosen models for baseline conditions can be used to demonstrate experimental and computational comparison in future research.

REFERENCES:

[1] Alozie, N. S., and Ganippa, L. C., 2019, "Diesel Exhaust Emissions and Mitigations," Introduction to Diesel Emissions, IntechOpen.
[2] Khair, M. K., and Majewski, W. A., 2006, Diesel Emissions and Their Control, SAE Technical Paper.
[3] How, H. G., Masjuki, H. H., Kalam, M. A., and Teoh, Y. H., 2018, "Influence of Injection Timing and Split Injection Strategies on Performance, Emissions, and Combustion Characteristics of Diesel Engine Fueled with Biodiesel Blended Fuels," Fuel, 213, pp. 106–114.
[4] Johnson, T., and Joshi, A., 2018, "Review of Vehicle Engine Efficiency and Emissions," SAE Int J Engines, 11(6), pp. 1307–1330.
[5] Abed, K. A., Gad, M. S., El Morsi, A. K., Sayed, M. M., and Elyazeed, S. A., 2019, "Effect of Biodiesel Fuels on Diesel Engine Emissions," Egyptian journal of petroleum, 28(2), pp. 183–188.

[6] Torelli, R., Scarcelli, R., Som, S., Zhu, X., Lee, S.-Y., Naber, J., Markt, D., and Raessi, M., 2019, "Toward Predictive and Computationally Affordable Lagrangian–Eulerian Modeling of Spray–Wall Interaction," International Journal of Engine Research, p. 146808741987061. https://doi.org/10.1177/1468087419870619.

[7] Wendt, J. F., Anderson, J. D., Degroote, J., Degrez, G., Dick, E., Grundmann, R., and Vierendeels, J., 2009, Computational Fluid Dynamics: An Introduction. https://doi.org/10.1007/978-3-540-85056-4.

[8] Turkel, E., 1983, "Progress in Computational Physics," Comput Fluids, 11(2), pp. 121–144.

[9] Date, A. W., 2005, Introduction to Computational Fluid Dynamics. https://doi.org/10.1017/CBO9780511808975.

[10] Lomax, H., Pulliam, T. H., Zingg, D. W., and Kowalewski, T. A., 2002, "Fundamentals of Computational Fluid Dynamics," Appl. Mech. Rev., 55(4), pp. B61–B61.

[11] Beale, J. C., and Reitz, R. D., 1999, "Modeling Spray Atomization with the Kelvin-Helmholtz/Rayleigh-Taylor Hybrid Model," Atomization and sprays, 9(6).

[12] Miya, M., Woodmansee, D. E., and Hanratty, T. J., 1971, "A Model for Roll Waves in Gas-Liquid Flow," Chem Eng Sci, 26(11), pp. 1915–1931.

[13] O'Rourke, P. J., and Amsden, A. A., 1987, The TAB Method for Numerical Calculation of Spray Droplet Breakup, SAE Technical Paper.

[14] Dukowicz, J. K., 1979, Quasi-Steady Droplet Phase Change in the Presence of Convection, Los Alamos Scientific Lab., NM (USA).

[15] Frolov, S. M., Frolov, F. S., and Basara, B., 2006, "Simple Model of Transient Drop Vaporization," Journal of Russian Laser Research, 27(6), pp. 562–574.

[16] Safiullah, Mahmud, R., Nishida, K., and Ogata, Y., 2020, "Experimental and Computational Study of Diesel Spray under Nonevaporating and Evaporating Conditions - Effects of Nozzle Hole Diameter and Injection Pressure," Atomization and Sprays, 30(9), pp. 627–649. https://doi.org/10.1615/AtomizSpr.2020034814.

[17] S. Som, D.E. Longman, A.I. Ramírez, S.K. Aggarwal (2010), "A comparison of injector flow and spray characteristics of biodiesel with petrodiesel," Fuel, 89, pp 4014–4024.

Appendix

Core Injection Primary Breakup Model		
Constant	Value	
C1	0	
C2	0	
C3	0	
C4	0	
C5	0	
C6	0	
C7	0.45	
C8	0.27	
C9	0.9	
C10	0.87	
C11	0.00008	
KHRT Secondary Breakup Model		
Constant	Default	Recommended

C1	0.61	0.61
C2	12	5-60
C3	10	10
C4	5.33	5.33
C5	1	1
C6	0.3	0.3
C7	0.05	0.05
C8	0.188	0.188

WAVE Secondary Breakup Model	
Constant	Value
C1	0.61
C2	30
C3	1
C4	0
C5	0
C6	0
C7	0
C8	0

TAB Secondary Breakup Model	
Constant	Value
C1	1
C2	2
C3	0
C4	3.3333
C5	8
C6	0.5
C7	10
C8	0.333
0.9	1